

REPORT DOCUMENTATION PAGE

Form Approved
OPM No. 0704-0188

Public reporting burden for this collection of information is estimated to average 1 hour per response, including the time for reviewing instructions, searching existing data sources, gathering and maintaining the data needed, and reviewing the collection of information. Send comments regarding this burden estimate or any other aspect of this collection of information, including suggestions for reducing this burden, to Washington Headquarters Services, Directorate for Information Operations and Reports, 1215 Jefferson Davis Highway, Suite 1204, Arlington, VA 22202-4302, and to the Office of Information and Regulatory Affairs, Office of Management and Budget, Washington, DC 20503.

1. AGENCY USE ONLY (Leave blank)		2. REPORT DATE 2/28/96	3. REPORT TYPE AND DATES COVERED Technical	
4. TITLE AND SUBTITLE Near field scattering through and from 2-D fluid-fluid rough interface			5. FUNDING NUMBERS Grant N00014-94-1-0068	
6. AUTHOR(S) John E. Moe and Darrell R. Jackson				
7. PERFORMING ORGANIZATION NAME(S) AND ADDRESS(ES) Applied Physics Laboratory University of Washington 1013 NE 40th Street Seattle, WA 98105-6698			8. PERFORMING ORGANIZATION REPORT NUMBER Submitted to J. Acoust. Soc. Am.	
9. SPONSORING / MONITORING AGENCY NAME(S) AND ADDRESS(ES) Office of Naval Research Ballston Tower 1 800 North Quincy Street Arlington, VA 22217-5660			10. SPONSORING / MONITORING AGENCY REPORT NUMBER	
11. SUPPLEMENTARY NOTES				
12a. DISTRIBUTION / AVAILABILITY STATEMENT Unlimited			12b. DISTRIBUTION CODE	
13. ABSTRACT (Maximum 200 words) General analytical expressions for the time dependent field intensity scattered from or through (penetrating) a 2-D fluid-fluid rough surface due to a narrowband incident plane wave, and a narrowband point source area derived and expressed in terms of the bistatic scattering cross section per unit area of the rough surface. Even though the cross-section is defined as a far-field entity, this near-field result is general and exact for the special case of a continuous wave (CW) source and incident plane wave. Dispersion of a pulse is a function of medium parameters, the incident and scattered directions, as well the bandwidth and center frequency of the source signal. First-order perturbation calculations for the case of a Gaussian pulse illustrate intensity pulse dispersion effects due to forward scattering into a lossy sediment. For the case of incidence below the critical grazing angle, first-order perturbation computations also show that the field scattered through a rough surface can be much greater than the zero-order field transmitted below the corresponding flat-surface depending on loss, and receiver depth to source wavelength ratio. These computations for the incoherent intensity penetrating the rough interface are compared to the flat-surface result, for both plane wave and point sources.				
14. SUBJECT TERMS near field scattering, first-order perturbation, 2-D fluid-fluid rough interface, penetration into sediments			15. NUMBER OF PAGES 36	
			16. PRICE CODE	
17. SECURITY CLASSIFICATION OF REPORT Unclassified	18. SECURITY CLASSIFICATION OF THIS PAGE Unclassified	19. SECURITY CLASSIFICATION OF ABSTRACT Unclassified	20. LIMITATION OF ABSTRACT SAR	

NEAR FIELD SCATTERING THROUGH AND FROM A 2-D FLUID-FLUID ROUGH INTERFACE

John E. Moe and Darrell R. Jackson (2/28/96)

*Applied Physics Laboratory, College of Ocean and Fishery Sciences, Department of
Electrical Engineering, University of Washington, Seattle, Washington. 98105*

General analytical expressions for the time dependent field intensity scattered from or through (penetrating) a 2-D fluid-fluid rough surface due to a narrowband incident plane wave, and a narrowband point source are derived and expressed in terms of the bistatic scattering cross section per unit area of the rough surface. Even though the cross-section is defined as a far-field entity, this near-field result is general and exact for the special case of a continuous wave (CW) source and incident plane wave. Dispersion of a pulse is a function of medium parameters, the incident and scattered directions, as well the bandwidth and center frequency of the source signal. First-order perturbation calculations for the case of a Gaussian pulse illustrate intensity pulse dispersion effects due to forward scattering into a lossy sediment. For the case of incidence below the critical grazing angle, first-order perturbation computations also show that the field scattered through a rough surface can be much greater than the zero-order field transmitted below the corresponding flat-surface depending on loss, and receiver depth to source wavelength ratio. These computations for the incoherent intensity penetrating the rough interface are compared to the flat-surface result, for both plane wave and point sources.

PACS numbers: 43.30.Hw, 43.30.Ma, 43.20.Fn

19960311 191

DISCLAIMER NOTICE



**THIS DOCUMENT IS BEST
QUALITY AVAILABLE. THE
COPY FURNISHED TO DTIC
CONTAINED A SIGNIFICANT
NUMBER OF PAGES WHICH DO
NOT REPRODUCE LEGIBLY.**

I. INTRODUCTION

Intermodal dispersion in a waveguide results in widening of the original transmitted pulse. Analogously, multiple arrivals of average signal energy due to rough surface scattering result in dispersion of the transmitted pulse. An additional source of pulse dispersion in a waveguide is the frequency dependence of the propagation constant. Similarly, frequency dependence of the propagation constant results in additional dispersion of the time dependent scattered field -- especially at shallow grazing angles. By assuming an arbitrary narrowband plane wave source signal, a general near-field expression for the time dependent scattered intensity is obtained in terms of statistics of the rough surface T -matrix, and equivalently, in terms of the scattering cross section. Thus, a near-field result is expressed in terms of a far-field entity, the scattering cross section. This result is then used to obtain an approximate scattered field expression for a point source. These results apply to both scattering from the interface as well as scattering through the interface. The latter case is of interest in bottom penetrating sonar.

Although the theoretical results are general in that they depend only on the interface T -matrix statistics, calculations are carried out using first-order perturbation theory for penetration examples. When the grazing angle of the incident field is below the critical angle in relation to the mean surface, only the zero-order component of the transmitted field is evanescent; the higher order components contain downward traveling waves (Moe and Jackson, 1994b). Acoustic intensity as a function of depth is computed and displayed for a continuous wave (CW) incident plane wave. The resulting profiles of intensity versus depth are compared with the flat-surface case. The time-dependent incoherent intensity is computed and displayed for a narrowband point source. These computations are carried out using a low-frequency cutoff for the bottom relief spectrum, and compared to the flat-surface case.

II. SCATTERING PROBLEM BACKGROUND

The general scattering geometry is shown in Fig. 1. An arbitrary pressure field, $\psi_i(\mathbf{r})$, is incident on a 2-D rough interface separating the homogenous lossless fluid in medium 1 (water), from the lossy fluid in medium 2 (sediment). The zero-mean rough surface is defined by:

$$z = hf(\mathbf{R}), \quad (1)$$

where \mathbf{R} is the transverse component of the three-dimensional position vector \mathbf{r} , and h is the root mean square (RMS) height of the surface. The total field, $\psi_1(\mathbf{r})$, above the rough surface is a sum of an arbitrary incident field, $\psi_i(\mathbf{r})$, and the resulting scattered pressure field, $\psi_f(\mathbf{r})$:

$$\psi_1(\mathbf{r}) = \psi_i(\mathbf{r}) + \psi_f(\mathbf{r}). \quad (2)$$

The boundary conditions consist of the continuity of pressure:

$$\psi_1 = \psi_2, \quad (3)$$

and the continuity of normal velocity:

$$\frac{1}{\rho_1} \hat{n} \cdot \nabla \psi_1 = \frac{1}{\rho_2} \hat{n} \cdot \nabla \psi_2 \quad (4)$$

where \hat{n} is normal to the surface, ρ_1 is the density of the water, and ρ_2 is the density of the sediment. The scattered field, $\psi_f(\mathbf{r})$, in the region above the highest point on the surface, and the incident field, are expressed in terms of the following (Weyl) plane wave expansions (Devaney and Sherman, 1973):

$$\psi_f(\mathbf{r}) = \int d^2K \Psi_f(\mathbf{K}) e^{ik_1\beta_1(\mathbf{K})z} e^{i\mathbf{K} \cdot \mathbf{R}} \quad (5)$$

and

$$\psi_i(\mathbf{r}) = \int d^2K \Psi_i(\mathbf{K}) e^{-ik_1\beta_1(\mathbf{K})z} e^{i\mathbf{K} \cdot \mathbf{R}}, \quad (6)$$

where \mathbf{K} is the two-dimensional transverse wave vector with magnitude K , k_1 is the wave number in the medium above the surface, and $k_1\beta_1$, is the z -component of the corresponding three-dimensional wave vector, with

$$\beta_1(\mathbf{K}) = \sqrt{1 - K^2 / k_1^2}. \quad (7)$$

For the continuous wave case, a factor of $e^{-i\omega t}$ is suppressed, but in general, the above equations are the Fourier transforms of the time domain field,

$$\psi_1(\mathbf{r}) \equiv \psi_1(\mathbf{r}, \omega) = \int dt \psi_1(\mathbf{r}, t) e^{i\omega t}. \quad (8)$$

The field below the rough surface is expressed as a plane wave expansion of waves traveling in the negative z direction,

$$\psi_{2-}(\mathbf{r}) = \int d^2K \Psi_{2-}(\mathbf{K}) e^{-ik_2\beta_2(\mathbf{K})z} e^{i\mathbf{K} \cdot \mathbf{R}}, \quad z < 0 \quad (9)$$

where,

$$\beta_2(\mathbf{K}) = \sqrt{1 - K^2 / k_2^2} \quad (10)$$

and

$$k_2 = k_1 \frac{1 + i\delta}{v} \quad (11)$$

is the complex wave number in the lossy medium below the surface with loss parameter, δ . The speed ratio, v , is the ratio of the sound speed in the sediment to the sound speed in the water. The scattered field can be expressed in terms of the incident field and the T -matrix, T_{11} :

$$\Psi_f(\mathbf{K}) = \int d^2K' T_{11}(\mathbf{K}, \mathbf{K}') \Psi_i(\mathbf{K}') \quad (12)$$

Likewise, the downward component of the scattered field penetrating below the surface is expressed in terms of the T -matrix, T_{12} :

$$\Psi_{2-}(\mathbf{K}) = \int d^2K' T_{12}(\mathbf{K}, \mathbf{K}') \Psi_i(\mathbf{K}'). \quad (13)$$

The scattered field for the case of an incident plane wave is found by substituting,

$$\Psi_i(\mathbf{K}) = \delta(\mathbf{K} - \mathbf{K}_i), \quad (14)$$

into Eq. (12), and the result into Eq. (5), yielding

$$\psi_f(\mathbf{r}) = \int d^2K T_{11}(\mathbf{K}, \mathbf{K}_i) e^{ik_1\beta_1(\mathbf{K})z} e^{i\mathbf{K} \cdot \mathbf{R}}. \quad (15)$$

The scattered field penetrating the surface for the incident plane wave case is found in the same way from Eqs. (9), (13) and (14),

$$\psi_{2-}(\mathbf{r}) = \int d^2K T_{12}(\mathbf{K}, \mathbf{K}_i) e^{-ik_2\beta_2(\mathbf{K})z} e^{i\mathbf{K} \cdot \mathbf{R}} \quad (16)$$

III. GENERAL RESULT FOR INCIDENT PLANE WAVE

The purpose of this section is to derive an expression for the average intensity time series at the receiver position, \mathbf{r} , due to a narrowband plane wave source. Although the following derivation considers the more general case of scattering *through* the rough interface, it also applies to scattering *from* a rough interface.

A. Time domain received signal

A narrowband source signal $s(t)$, with Fourier transform:

$$S(\omega) = \int_{-\infty}^{\infty} dt s(t) e^{i\omega t}, \quad (17)$$

can be represented as:

$$s(t) = \text{Re} \left\{ u(t) e^{-i\omega_c t} \right\}, \quad (18)$$

where $u(t)$ is the corresponding complex baseband input signal, with Fourier transform, $U(\omega)$, and ω_c is the carrier frequency, or center frequency of the pulse. An incident plane wave pulse with direction denoted by the transverse unit vector, $\hat{\alpha}_i$, and incident grazing angle θ_i , is expressed in terms of its 2-D Fourier transform as:

$$\Psi_i(\mathbf{K}, \omega) = S(\omega) \delta(\mathbf{K} - \mathbf{K}_i) e^{i\omega z_s \sin \theta_i / c_1}, \quad \omega > 0, \quad (19)$$

where

$$\mathbf{K}_i = \frac{\omega}{c_1} \cos \theta_i \hat{\alpha}_i, \quad (20)$$

is the incident transverse wave vector, and z_s is taken to be an arbitrary source height. Using Eqs. (9), (13), (17), (18), (19), and chapter 3, Proakis (1989), the baseband pressure signal $\psi_{bb}(\mathbf{r}, t)$ at a position $\mathbf{r} = (\mathbf{R}, z)$ below the surface is expressed as:

$$\psi_{bb}(\mathbf{r}, t) = \frac{1}{2\pi} \int d\omega' \left\{ U(\omega') e^{-i\omega' t} \int d^2K T_{12}(\mathbf{K}, \mathbf{K}_i, \omega' + \omega_c) \right. \\ \left. \times e^{i \sin \theta_i z_s (\omega' + \omega_c) / c_1} e^{-i\kappa \beta_2(K, \omega' + \omega_c) z (\omega' + \omega_c) / c_1} e^{i\mathbf{K} \cdot \mathbf{R}} \right\}, \quad (21)$$

where

$$\kappa \equiv k_2 / k_1 \quad (22)$$

is the complex wave number ratio,

$$\mathbf{K}_i = \frac{\omega + \omega_c}{c_1} \cos \theta_i \hat{\alpha}_i, \quad (23)$$

and we have explicitly shown the dependence of $\beta_2(\mathbf{K})$ on frequency as well as on the magnitude of \mathbf{K} .

B. Time dependent intensity

The time dependent intensity at position \mathbf{r} can be expressed as:

$$I_2(\mathbf{r}, t) = \left\langle |\psi_{bb}(\mathbf{r}, t)|^2 \right\rangle, \quad (24)$$

Combining Eqs. (21) and (24) yields:

$$\begin{aligned} I_2(\mathbf{r}, t) = & \left(\frac{1}{2\pi} \right)^2 \int d\omega' \int d\omega'' \left\{ U(\omega') U^*(\omega'') e^{-i\omega' t} e^{i\omega'' t} \right. \\ & \times \int d^2 K'' \int d^2 K' \left\langle T_{12}(\mathbf{K}', \mathbf{K}'_i, \omega' + \omega_c) T_{12}^*(\mathbf{K}'', \mathbf{K}''_i, \omega'' + \omega_c) \right\rangle \\ & \times e^{i\mathbf{K}' \cdot \mathbf{R}_e} e^{-i\mathbf{K}'' \cdot \mathbf{R}_e} e^{i \sin \theta_i z_s \omega' / c_1} e^{-i \sin \theta_i z_s \omega'' / c_1} \\ & \times e^{-i \kappa \beta_2 (K', \omega' + \omega_c) z(\omega' + \omega_c) / c_1} e^{i (\kappa \beta_2 (K'', \omega'' + \omega_c))^* z(\omega'' + \omega_c) / c_1} \left. \right\} \end{aligned} \quad (25)$$

where the transverse wave vectors for the incident field at the angular frequencies ω'' , and ω' are

$$\mathbf{K}''_i = \frac{\omega_c + \omega''}{c_1} \cos \theta_i \hat{\alpha}_i, \quad \mathbf{K}'_i = \frac{\omega_c + \omega'}{c_1} \cos \theta_i \hat{\alpha}_i. \quad (26)$$

Define $C_{12}(\mathbf{K}', \mathbf{K}'', \mathbf{K}'_i, \mathbf{K}''_i, \omega_c + \omega', \omega_c + \omega'')$, (see for example Zipfel and DeSanto, 1972; Voronovich, 1995) such that

$$\begin{aligned} & \left\langle T_{12}(\mathbf{K}', \mathbf{K}'_i, \omega' + \omega_c) T_{12}^*(\mathbf{K}'', \mathbf{K}''_i, \omega'' + \omega_c) \right\rangle \\ & \equiv C_{12}(\mathbf{K}', \mathbf{K}'', \mathbf{K}'_i, \mathbf{K}''_i, \omega_c + \omega', \omega_c + \omega'') \delta(\mathbf{K}'' - \mathbf{K}' + \mathbf{K}'_i - \mathbf{K}''_i) \end{aligned} \quad (27)$$

In the above expression, the subscript i is used to represent scattering into the sediment and the dependence of T_{12} on ω is included in the argument. Substituting Eq. (27) and

$$\mathbf{K}''_i - \mathbf{K}'_i = \frac{\omega'' - \omega'}{c_1} \cos \theta_i \hat{\alpha}_i \equiv \mathbf{K}_d \quad (28)$$

into Eq. (25), and changing the integration variable \mathbf{K}' to

$$\mathbf{K} = \mathbf{K}' + \mathbf{K}_d / 2, \quad (29)$$

yields:

$$\begin{aligned}
I_2(\mathbf{r}, t) = & \left(\frac{1}{2\pi} \right)^2 \int d\omega' \int d\omega'' U(\omega') U^*(\omega'') e^{-i\omega' t} e^{i\omega'' t} \\
& \times \int d^2 K G_{12}(\mathbf{K} - \mathbf{K}_d/2, \mathbf{K} + \mathbf{K}_d/2, \mathbf{K}'_i, \mathbf{K}''_i, \omega_c + \omega', \omega_c + \omega'') e^{-i\mathbf{K}_d \cdot \mathbf{R}} \\
& \times e^{i \sin \theta_i z_s \omega' / c_1} e^{-i \sin \theta_i z_s \omega'' / c_1} \\
& \times e^{-i \kappa \beta_2 (|\mathbf{K} - \mathbf{K}_d/2|, \omega_c + \omega') z \omega' / c_1} e^{i \kappa \beta_2 (|\mathbf{K} + \mathbf{K}_d/2|, \omega_c + \omega'')^* z (\omega_c + \omega'') / c_1}
\end{aligned} \tag{30}$$

Equation (30) is now evaluated by making a few approximations. For the case of a narrowband source signal, we can assume G_{12} is a slowly varying function of frequency,

$$\begin{aligned}
G_{12}(\mathbf{K} - \mathbf{K}_d/2, \mathbf{K} + \mathbf{K}_d/2, \mathbf{K}'_i, \mathbf{K}''_i, \omega_c + \omega'', \omega_c + \omega') & \cong G_{12}(\mathbf{K}, \mathbf{K}, \mathbf{K}_i, \mathbf{K}_i, \omega_c, \omega_c) \\
& \equiv G_{12}(\mathbf{K}, \mathbf{K}_i, \omega_c)
\end{aligned} \tag{31}$$

where the relation (Thorsos and Jackson, 1989; Berman, 1992),

$$G_{12}(\mathbf{K}, \mathbf{K}_i, \omega_c) \delta(\mathbf{K} - \mathbf{K}'') \equiv \langle T_{12}(\mathbf{K}, \mathbf{K}_i, \omega_c) T_{12}^*(\mathbf{K}'', \mathbf{K}_i, \omega_c) \rangle \tag{32}$$

is a special case of Eq. (27), and \mathbf{K}_i is evaluated at the center frequency:

$$\mathbf{K}_i = \frac{\omega_c}{c_1} \cos \theta_i \hat{\alpha}_i. \tag{33}$$

First-order perturbation theory can be used to show that Equation (31) is a valid approximation. Also, define the vertical component of the wave vector in medium 2,

$$B_2(K, \omega_c + \omega', \omega_c + \omega'') \equiv ((\omega_c + \omega')/c_1) \kappa \beta_2 (|\mathbf{K} - \mathbf{K}_d/2|, \omega_c + \omega'), \tag{34}$$

Analytical expressions for dispersion in a waveguide can be found by expanding the exponent of the time dependent field in a power series (for example, see Ishimaru, 1991). Since $K_d = |\mathbf{K}_d|$ is a function of both ω' and ω'' , $(\omega'/c_1) \kappa \beta_2$ is expanded in a power series in ω' and ω'' , for the case of a narrowband signal:

$$B_2(K, \omega_c + \omega', \omega_c + \omega'') \equiv B_{2c}(K) + \frac{\partial B_2}{\partial \omega'} \omega' + \frac{\partial B_2}{\partial \omega''} \omega'' + \frac{1}{2} \left[\frac{\partial^2 B_2}{\partial \omega'^2} \omega'^2 + 2 \frac{\partial^2 B_2}{\partial \omega' \partial \omega''} \omega' \omega'' + \frac{\partial^2 B_2}{\partial \omega''^2} \omega''^2 \right] \quad (35)$$

where the derivatives are evaluated at $\omega' = \omega'' = 0$, and

$$B_{2c}(K) \equiv \kappa k_1 \beta_2(K, \omega_c), \quad (36)$$

where the wave number, k_1 , in the above equation, and all following equations, is evaluated at the center frequency ($k_1 = \omega_c / c_1$). Solving for the derivatives in Eq. (35) and combining like powers of ω' and ω'' in Eq. (30) yields,

$$I_2(\mathbf{r}, t) \equiv \int d^2K \left\{ C_{12}(\mathbf{K}, \mathbf{K}_i, \omega_c) e^{2k_{1c} \text{Im}(\kappa \beta_2(K, \omega_c))z} \times \frac{1}{2\pi} \int d\omega'' U^*(\omega'') e^{i\omega''(t-t_1-t_2)^*} e^{i\omega''^2 P^*/4} \times \frac{1}{2\pi} \int d\omega' U(\omega') e^{-i\omega'(t-t_1-t_2)} e^{-\omega' \omega'' Q} e^{-i\omega'^2 P/4} \right\} \quad (37)$$

where

$$t_1 = \frac{\mathbf{R} \cdot \hat{\alpha}_i}{c_1} \cos \theta_i + \frac{z_s}{c_1} \sin \theta_i + z \frac{\hat{\alpha}_i \cdot \mathbf{K} \cos \theta_i}{c_1 k_1} \text{Re} \left(\frac{1}{\kappa \beta_2(K, \omega_c)} \right). \quad (38)$$

and

$$t_2 = \frac{-z \kappa / c_1}{\beta_2(K, \omega_c)}. \quad (39)$$

The physical significance of these parameters will be discussed later. Note that t_1 is real and t_2 is complex. The complex coefficient

$$P = \left\{ \left(2\kappa^2 / B_{2c}^3 \right) \left(\hat{\alpha}_i \cdot \mathbf{K} \omega_c \cos \theta_i / c_1^3 - (K/c_1)^2 \right) - i \text{Im}(1/B_{2c}) (\cos \theta_i / c_1)^2 - i \text{Im}(1/B_{2c}^3) (\hat{\alpha}_i \cdot \mathbf{K} \cos \theta_i / c_1)^2 \right\} z \quad (40)$$

and the real coefficient

$$Q = \text{Im} \left\{ \left(\hat{\alpha}_i \cdot \mathbf{K} \cos \theta_i / B_{2c}^3 \right) \left(\kappa^2 \omega_c / c_1^3 - \hat{\alpha}_i \cdot \mathbf{K} \cos \theta_i / (2c_1^2) \right) - \cos^2 \theta_i / (2c_1^2 B_{2c}) \right\} z \quad (41)$$

lead to pulse dispersion. Defining

$$g^2(t) \equiv \frac{1}{2\pi} \int d\omega'' U^*(\omega'') e^{i\omega'' t^*} e^{i\omega''^2 P^*/4} \\ \times \frac{1}{2\pi} \int d\omega' U(\omega') e^{-i\omega' t} e^{-i\omega' \omega'' Q} e^{-i\omega'^2 P/4} \quad (42)$$

results in a simple expression for the time dependent intensity in medium 2:

$$I_2(\mathbf{r}, t) \equiv \int d^2 K C_{12}(\mathbf{K}, \mathbf{K}_i, \omega_c) e^{2k_1 \text{Im}(\kappa \beta_2(K, \omega_c))z} g^2(t - t_d). \quad (43)$$

In addition to being a function of the complex argument, t , $g(t)$ is a function of K , the incident field direction, and fluid-sediment parameters. Note that

$$t_d \equiv t_1 + t_2. \quad (44)$$

is also a complex function of K . For an arbitrarily small pulse bandwidth (CW), the dispersion terms are arbitrarily small, and $g(t) \rightarrow u(t)$.

While Eq. (43) involves an integral over the transverse wave vector, it can be converted to an integral over the scattering surface through the change of variable,

$$\mathbf{R}' = \mathbf{R} - v r_d \mathbf{K} / k_1. \quad (45)$$

As shown in Fig. 2, \mathbf{R}' is the location of a small scattering patch on the surface, and $r_d = |\mathbf{r}_d|$ is the distance from this patch to the field point, \mathbf{r} ,

$$r_d = \sqrt{|\mathbf{R} - \mathbf{R}'|^2 + z^2} \quad (46)$$

As the variables R'_x and R'_y range over all real values, Eq. (45) constrains \mathbf{K} to the range $K < k_1/v$. This change of variables forces neglect of evanescent waves.

The Jacobian follows from Eq. (45),

$$\left(\frac{\partial K}{\partial R'}\right) = \frac{k_1^2}{v^2 r_d^6} \begin{vmatrix} y_d^2 + z^2 & x_d y_d \\ x_d y_d & x_d^2 + z^2 \end{vmatrix} = \frac{k_1^2}{v^2 r_d^4} z^2, \quad (47)$$

where x_d , and y_d are the transverse coordinates of \mathbf{r}_d . The geometric significance of these definitions is apparent when one assumes that the loss parameter is small ($\delta \ll 1$), Then

$$\begin{aligned} k_1 \kappa \beta_2(K, \omega_c) &= \sqrt{(\kappa k_1)^2 - K^2} \\ &\equiv (k_1 \sin \theta_2 / v) (1 + i\delta / \sin^2 \theta_2) \end{aligned} \quad (48)$$

where

$$\sin \theta_2 = \sqrt{1 - K^2 v^2 / k_1^2} = |z| / r_d \quad (49)$$

is the sine of the scattered grazing angle defined in Fig. 2. Dropping terms of second order and higher in the loss parameter, the significance of t_1 and t_2 becomes apparent, as

$$t_1 = \mathbf{R}' \cdot \hat{\alpha}_i \cos \theta_i / c_1 + z_s \sin \theta_i / c_1 \quad (50)$$

is the time required for the incident plane wave front with direction $(\hat{\alpha}_i \cos \theta_i, \sin \theta_i)$ to travel from the source reference point, $(0, 0, z_s)$ to the scattering patch, $(\mathbf{R}', 0)$, and

$$\text{Re}(t_2) = r_d / c_2 \quad (51)$$

is the time required for a spherical wave scattered from the patch at $(\mathbf{R}', 0)$ to travel through the sediment to the field point (\mathbf{R}, z) , $z < 0$. According to Eq. (48), the absorption exponent in medium 2 is given by

$$\text{Im}(k_1 \kappa \beta_2(K, \omega_c)) |z| = \frac{k_1 \delta}{v} |z| / \sin \theta_2 = \text{Im}(k_2) r_d. \quad (52)$$

Substituting Eqs. (47) and (52) into Eq. (43) results in:

$$\langle |\psi_{2-}(\mathbf{r})|^2 \rangle = \int d^2R' \frac{k_1^2 \sin^2(\theta_2)}{v^2 r_d^2} C_{12}(\mathbf{K}, \mathbf{K}_i, \omega_c) e^{-2\text{Im}(k_2)r_d} g^2(t-t_d). \quad (53)$$

Substituting the following quantity,

$$\sigma_{12}(\hat{\alpha}, \hat{\alpha}_i) \equiv \frac{k_1^2 \sin^2(\theta_2)}{v^2} C_{12}(\mathbf{K}, \mathbf{K}_i, \omega_c), \quad (54)$$

$$\hat{\alpha} = \mathbf{K}/K, \text{ and } \hat{\alpha}_i = \mathbf{K}_i/K_i \quad (55)$$

into Eq. (53) yields,

$$I_2(\mathbf{r}, t) \equiv \int d^2R' \frac{\sigma_{12}(\hat{\alpha}, \hat{\alpha}_i)}{|\mathbf{r} - \mathbf{r}'|^2} e^{-2\text{Im}(k_2)|\mathbf{r} - \mathbf{r}'|} g^2(t-t_d). \quad (56)$$

The interpretation of σ_{12} as a scattering cross section will be justified later in this section. Since $\mathbf{K} = k_1(\mathbf{R} - \mathbf{R}')/(vr_d)$, t_1 , t_2 , g , and therefore P , and Q are functions of $|\mathbf{R} - \mathbf{R}'|$. Limiting the integration in Eq. (43) to the non-evanescent regions, $K < k_1/v$, noticeably affects the integral only when within a wavelength of the surface. Note that the CW result follows from Eq. (56) by simply setting $g(t-t_d) = 1$. For this case of an arbitrarily narrowband source signal, the result in Eq. (43) is exact, and Eq. (56) is exact everywhere, except very close to the surface.

Although the intensity of the field scattered into the water, $I_1(\mathbf{r}, t)$, is similarly derived, the corresponding expression for $I_1(\mathbf{r}, t)$ is most easily obtained as a special case of Eq. (56) by substituting medium 1 parameters for medium 2 parameters. For example, k_1 is substituted for k_2 , β_1 for $\kappa\beta_2$, etc. For this special case, Eq. (56) simplifies to

$$I_1(\mathbf{r}, t) \equiv \int d^2R' \frac{\sigma_{11}(\hat{\alpha}, \hat{\alpha}_i)}{|\mathbf{r} - \mathbf{r}'|^2} g_{11}^2(t-t_d), \quad (57)$$

where from Eq. (54)

$$\sigma_{11}(\hat{\alpha}, \hat{\alpha}_i) = k_1^2 \sin^2(\theta_2) |G_{11}(\mathbf{K}, \mathbf{K}_i, \omega_c)|^2. \quad (58)$$

In this case, θ_2 is also the scattered field grazing angle measured from the mean horizontal plane, $|z|/r_d = \sin(\theta_2)$. Again, the quantity G_{11} is found from the relation (Eq. 32)

$$G_{11}(\mathbf{K}, \mathbf{K}_i, \omega_c) \delta(\mathbf{K} - \mathbf{K}'') \equiv \langle T_{11}(\mathbf{K}, \mathbf{K}_i, \omega_c) T_{11}^*(\mathbf{K}'', \mathbf{K}_i, \omega_c) \rangle \quad (59)$$

There is no loss in this case -- $Q = 0$, and therefore,

$$g_{11}^2(t) \equiv \left| \frac{1}{2\pi} \int d\omega' U(\omega') e^{-i\omega' t} e^{-i\omega'^2 R_{11}/4} \right|^2, \quad (60)$$

$$R_{11} \equiv \left(2/B_{11c}^3 \right) \left(\omega_c K \cos \theta_i \cos \phi / c_1^3 - (K/c_1)^2 \right), \quad (61)$$

and

$$B_{1c}(K) \equiv k_1 \beta_1(K, \omega_c). \quad (62)$$

Note that t_d is still given by Eq. (44), but the propagation time from the surface patch to the receiver, or observation point above the surface is a real quantity --

$$t_2 = \frac{z/c_1}{\beta_1(K, \omega_c)}. \quad (63)$$

As shown in Voronovich (1995), the quantity $\sigma_{11}(\hat{\alpha}, \hat{\alpha}_i)$ in Eq. (58) is actually the scattering cross section per unit area defined in Ishimaru, (1978).

$$\sigma_{11}(\hat{\alpha}, \hat{\alpha}_i) = \frac{|\mathbf{r} - \mathbf{r}'|^2}{\Delta A} \frac{\langle |\psi_f|^2 \rangle}{|\psi_i|^2}, \quad (64)$$

where ψ_i is a plane-wave field incident on a surface patch of area ΔA , and $\hat{\alpha}_i$ is the unit vector in the direction of propagation of the incident field; ψ_f is the scattered field

at a long distance $|\mathbf{r}-\mathbf{r}'|^2$ from the surface, in the direction denoted by the unit vector, $\hat{\alpha}$. Similarly, σ_{12} , is the scattering cross section per unit area of a rough surface relating the incident field intensity to the scattered field intensity in medium 2 (the sediment), defined as:

$$\sigma_{12}(\hat{\alpha}, \hat{\alpha}_i) = \frac{|\mathbf{r}-\mathbf{r}'|^2}{\Delta A} \frac{\langle |\psi_{2-}|^2 \rangle}{|\psi_i|^2} e^{2\text{Im}(k_2)|\mathbf{r}-\mathbf{r}'|}, \quad (65)$$

where ψ_{2-} is the field at the receiver in the sediment, a distance $|\mathbf{r}-\mathbf{r}'|$ from the surface patch, and the unit vector $\hat{\alpha}$ represents the transverse direction of the scattered field in the lower medium. The result given in Eq. (56) (or Eq. 57) is remarkable, as the cross section, Eq. (65), is a far-field entity. Close inspection of Eq. (56) shows that it is the "naive" sonar equation, when $u(t)$ is substituted for $g(t)$, in which the scattering intensity is obtained by integrating the bistatic cross section over the interface with appropriate attenuation due to spreading and sediment loss. Equations (32) and (54) are a convenient way to find σ_{12} in theoretical developments; Eqs. (58) and (59) are a convenient way to find σ_{11} .

C. Dispersion of a Gaussian input pulse

Two types of pulse dispersion occur in this problem. One type is simply due to scattering and is treated by the integral in Eq. (56) over the scattering surface. The other type of dispersion is due to the frequency dependence of the propagation constant, and is embodied in Eqs. (42). This subsection focuses on this form of dispersion. Consider the case of an input pulse with a Gaussian envelope,

$$u(t) = e^{-t^2/t_s^2}, \quad (66)$$

with Fourier transform

$$U(\omega) = t_s \sqrt{\pi} e^{-t_s^2 \omega^2 / 4}. \quad (67)$$

Substituting Eq. (67) into Eq. (42) and integrating over ω' and ω'' yields:

$$g^2(t) = \frac{t_s^2}{q' q''} e^{-t^2 / q'^2} e^{-\left(t^* + 2tQ/q'^2\right)^2 / q''^2}, \quad (68)$$

where

$$q' \equiv \sqrt{t_s^2 + iP}, \quad (69)$$

$$q'' \equiv \sqrt{t_s^2 - iP''}, \quad (70)$$

and

$$P'' \equiv P^* - i(2Q/q')^2, \quad (71)$$

Substituting Eqs. (69) and (70) into Eq. (68), and simplifying, yields an expression equivalent to Eq. (68)

$$g^2(t) = \frac{t_s^2}{\sqrt{|t_s^2 - iP^*|^2 - (2Q)^2}} \exp \left(\frac{-2 \operatorname{Re} \left\{ (t_s^2 - iP^*) t^2 \right\}}{|t_s^2 - iP^*|^2 - (2Q)^2} \right), \quad (72)$$

As mentioned, $\operatorname{Re}(t_d) = \operatorname{Re}(t_2) + t_1$ represents the propagation delay of the pulse. The imaginary part of t_2 is a result of modeling the sediment as lossy. Since higher frequency signals are attenuated more than lower frequency signals, the lower frequency components of a narrowband signal will be less attenuated than the center frequency. The imaginary component of t_2 , along with Q , and the imaginary component of P compensate for typically excessive loss in the CW loss term -- the exponential term in Eq. (43) or Eq. (56). In addition, P is a frequency dispersion term that results in pulse broadening of the signal below the rough surface (specifically the real component of P). Note that for the zero loss case, the parameter $Q = 0$. The

effect of loss and the parameters P and Q is seen in Fig. 3 for $g(t-t_d)$ from Eq. (72) evaluated at

$$g^2(t-t_d)\Big|_{t=\text{Re}(t_d)} = g^2(-t_{2i}), \quad t_{2i} = \text{Im}(t_d) = \text{Im}(t_2) \quad (73)$$

and plotted as a function of scattered grazing angle for lossy and zero-loss sediment. In Fig. 3, the pulse length parameter, t_s , is equal to two periods of the center, or carrier frequency for both cases shown. When the loss and dispersion are small, $|g(-t_{2i})|$ approaches $u(0)=1$. The smaller the scattered grazing angle, the greater the dispersion, and the smaller one would expect the pulse peak amplitude. However, the loss of the CW signal represented by the term, $e^{-2\text{Im}(k_2)|\mathbf{r}-\mathbf{r}'|}$, is greater than the loss of the narrowband signal, and the propagation distance becomes large for small scattered grazing angles (z is fixed). Even though there is dispersion, the loss for the narrow band case is significantly less than the CW case, and $|g(-t_{2i})| > 1$. In the case of Fig. 3, with depth of 0.3 m, $|g(-t_{2i})|$ is greater than one for very small grazing angles since the propagation distance becomes very large. An example with zero loss always has $P'' = P^*$, $t_{2i} = 0$, and it is always true that $|g(0)| \leq 1$.

IV. ANALYTICAL SCATTERING MODEL (PERTURBATION THEORY)

In the examples of the following section, the intensity of the field in medium 2 is divided into coherent and incoherent parts. The incoherent intensity is treated using first-order perturbation theory, and the coherent intensity is treated in zeroth order - the flat surface solution is used. There is a slight inconsistency in this approach, in that the incoherent intensity is proportional to the second power of $k_1 h$, while the coherent intensity is only computed to an accuracy of zeroth order. As Rice (1951) has shown,

the coherent intensity to second order in $k_1 h$ is obtained by subtracting the power carried by the incoherent intensity. For small $k_1 h$, this correction is necessarily slight.

A. Incoherent intensity using the first-order perturbation approximation

In this section, the first-order perturbation results are given for the scattering cross section for insertion in Eq. (56). The first-order T -matrix is proportional to the 2-D Fourier transform of the surface, $F(\mathbf{K})$, (see the Appendix) and is given by:

$$T_{12}(\mathbf{K}, \mathbf{K}_i) \equiv (k_1 h) T_{12}^{(1)}(\mathbf{K}, \mathbf{K}_i) = (k_1 h) H_{12}(\mathbf{K}, \mathbf{K}_i) F(\mathbf{K} - \mathbf{K}_i), \quad (74)$$

where

$$H_{12}(\mathbf{K}'', \mathbf{K}) = \frac{\mathcal{T}(\mathbf{K}'')}{2i\beta_1(\mathbf{K}'')} \left[a(\mathbf{K}'', \mathbf{K})(1 + \Gamma(\mathbf{K})) - b(\mathbf{K}'', \mathbf{K})(1 - \Gamma(\mathbf{K})) \right]. \quad (75)$$

is a function of the flat-surface reflection coefficient, Γ , the flat-surface transmission coefficient,

$$\mathcal{T}(\mathbf{K}) = 1 + \Gamma(\mathbf{K}) \quad (76)$$

as well as the factors $a(\mathbf{K}'', \mathbf{K})$ and $b(\mathbf{K}'', \mathbf{K})$ defined in the appendix. Using

$$h^2 \langle F(\mathbf{K}'' - \mathbf{K}_i) F(\mathbf{K}' - \mathbf{K}_i) \rangle = W(\mathbf{K}' - \mathbf{K}_i) \delta(\mathbf{K}'' - \mathbf{K}') \quad (77)$$

together with Eq. (32), and Eq. (74) yields:

$$C_{12}(\mathbf{K}, \mathbf{K}_i, \omega_c) = |k_1 H_{12}(\mathbf{K}, \mathbf{K}_i)|^2 W(\mathbf{K} - \mathbf{K}_i). \quad (78)$$

An expression for the first-order incoherent intensity results from substituting Eq. (78) into Eq. (43). Equivalently, the first-order intensity is found from Eq. (56), where

$$\sigma_{12}^{(1)}(\hat{\alpha}_f, \hat{\alpha}_i) = \frac{k_1^2 \sin^2(\theta_2)}{v^2} |k_1 H_{12}(\mathbf{K}_f, \mathbf{K}_i)|^2 W(\mathbf{K}_f - \mathbf{K}_i), \quad (79)$$

the scattering cross section from first-order perturbation theory, is found from substituting Eq. (79) into Eq. (54). Although the cross section in this approximation is actually second order in $k_1 h$, (Thorsos and Jackson, 1989), we will refer to it as the first-order cross section, and will refer to the corresponding scattered intensity as the first-order intensity.

B. Zero-order intensity

The zero-order, or flat-surface transmitted coherent intensity for an incident plane wave, is given by the magnitude squared of Eq. (16), with $T_{12}^{(0)}(\mathbf{K}, \mathbf{K}_i)$ given by (A6):

$$\left| \psi_{2-}^{(0)}(\mathbf{r}) \right|^2 = \left| \mathcal{T}(\mathbf{K}_i) \right|^2 e^{\text{Im}(k_2 \beta_2(\mathbf{K}_i))z}. \quad (80)$$

C. Roughness spectrum

The two dimensional Gaussian random process $f(\mathbf{R})$ describing the seafloor surface is assumed to be isotropic, with a roughness spectrum, $W(\mathbf{K})$, in the form of a filtered power-law (Moe and Jackson, 1994b),

$$W(\mathbf{K}) = \frac{w_2}{K^\gamma} \left(1 - e^{-(Ka)^2/2} \right)^2, \quad (81)$$

with RMS height,

$$h = \sqrt{2\pi \int_0^\infty W(\mathbf{K}) K dK} = \sqrt{\frac{2\pi w_2 a^{\gamma-2}}{\gamma-2} \Gamma(2-\gamma/2) [2^{2-\gamma/2} - 1]}. \quad (82)$$

Here, Γ refers to the gamma function -- not the reflection coefficient. The factor $\left(1 - e^{-(Ka)^2/2} \right)^2$ is obtained by subtracting a Gaussian weighted moving average (Papoulis, 1984) of the surface from itself.

V. APPLICATIONS AND CALCULATIONS

Although the theoretical results in this paper are general and include scattering back into the water, the examples deal with scattering through a rough fluid-fluid interface ($z < 0$). Both plane-wave and point sources are considered, and the scattered intensity is computed for the flat-surface case.

A. Continuous plane wave source

The first-order intensity of the field penetrating through a rough surface, with roughness spectrum given in Eq. (82), due to a CW incident plane wave is calculated using Eqs. (78) in Eq. (43), and setting $g(t - t_d) = 1$. Using parameters appropriate to a sandy seafloor, the incoherent acoustic intensity is computed as a function of depth. Since the grazing angle in this example is below critical, the zero-order (flat-surface) field is evanescent. Near the surface, the incoherent intensity decays with increasing depth at rate comparable to the zero-order coherent intensity, but decays at a rate dictated by the sediment loss further from the surface. This example (Fig. 4) shows that roughness has a significant effect on the field transmitted through a surface.

B. Incoherent field due to a point source including dispersion

Expressing the 2-D integral in Eq. (56) in terms of a summation over the surface yields

$$I_2(\mathbf{r}, t) \equiv \Delta A \sum_n \frac{\sigma_n(\hat{\alpha}_{fn}, \hat{\alpha}_i)}{r_{2n}^2} g^2(t - t_{1n} - t_{2n}) e^{-2\text{Im}(k_2)r_{2n}}, \quad (83)$$

where

$$r_{2n} = |\mathbf{r} - \mathbf{r}'_n| \quad (84)$$

is the distance from surface patch n , at position \mathbf{r}'_n of size ΔA to the observed field point, \mathbf{r} , and

$$\hat{\alpha}_{fn} = \frac{\mathbf{R} - \mathbf{R}'}{|\mathbf{R} - \mathbf{R}'|}. \quad (85)$$

The propagation time from this surface patch to the receiver, $\text{Re}(t_{2n})$, is also given by:

$$\text{Re}(t_{2n}) = r_{2n}/c_2. \quad (86)$$

As the area of each surface patch, ΔA , approaches zero, the summation in Eq. (83) approaches the exact integral in Eq. (56).

An expression for the incoherent first-order field below the surface due to a point source follows from Eq. (83). Here, the surface patch (area ΔA) is chosen sufficiently small in relation to the distance r_{1n} from the point source to surface patch n , to insure that the field incident on the surface is a plane wave. The scattered or penetrating field intensity is given by:

$$I_2(\mathbf{r}, t) \equiv \Delta A \sum_n \frac{\sigma_n(\hat{\alpha}_{fn}, \hat{\alpha}_{in})}{r_{1n}^2 r_{2n}^2} g^2(t - t_{dn}) e^{-2\text{Im}(k_2)r_{2n}}, \quad (87)$$

where,

$$\hat{\alpha}_{in} = \frac{\mathbf{R}'_n - \mathbf{R}_s}{|\mathbf{R}'_n - \mathbf{R}_s|}, \quad (88)$$

and \mathbf{R}_s is the transverse coordinate vector of the source. The total propagation time is given by the real part of:

$$t_{dn} = \frac{r_{1n}}{c_1} + t_{2n}. \quad (89)$$

with

$$r_{1n} = \sqrt{|\mathbf{R}'_n - \mathbf{R}_s|^2 + z_s^2}. \quad (90)$$

When the approximation $g(t) = u(t)$ is made, Eq. (87) is in the form of a convolution, reducing the computation time significantly.

Using the expression for the first-order scattering cross-section given in Eq. (79), the approximate incoherent intensity pulse in lossy sediment below a rough surface due to a Gaussian narrowband point source above the surface is found for two cases. In Fig. 5a, the incoherent pulse time series at a position below a rough surface in a lossy medium due to a point source is found using Eq. (72) for $g^2(t)$ in Eq. (87), and is compared to the result obtained setting the dispersion terms P and Q to zero -- $g(t) = u(t)$. Although the resulting pulse shapes are close in magnitude, as well as peak arrival time, including the dispersion terms does result in an incoherent intensity pulse that has a smaller peak magnitude, and is wider than the approximation obtained by setting $g(t) = u(t)$. In this example, the parameter t_s in Eq. (66) is equal to two cycles of the center frequency of $f_c = 20\text{Khz}$. This frequency results in $k_1 h = 0.25$, which is within the region of accuracy for first-order perturbation theory (Thorsos and Jackson, 1989; Thorsos, 1990). In Fig. 5b, the point source is higher, but the incident angle is the same. In this example, including the dispersion parameters has a slightly greater effect.

C. Zero-order calculations

Setting

$$\Psi_{2-}(\mathbf{K}) = \mathcal{T}(\mathbf{K})\Psi_i(\mathbf{K}) \quad (91)$$

and

$$\Psi_i(\mathbf{K}) = \frac{i}{2\pi k_1 \beta_1(\mathbf{K})} e^{-i\mathbf{K} \cdot \mathbf{R}_s} e^{ik_1 \beta_1(\mathbf{K}) z_s} \quad (92)$$

in Eq. (9) results in an expression for the field penetrating a flat fluid-fluid interface due to a point source at (\mathbf{R}_s, z_s) with unit magnitude at 1m from the source. The resulting integral simplifies to:

$$\psi_{2-}(\mathbf{r}) = i \int_0^{\infty} dK \frac{K \mathcal{T}(\mathbf{K})}{k_1 \beta_1(\mathbf{K})} e^{i(z_s k_1 \beta_1(\mathbf{K}) - z k_2 \beta_2(\mathbf{K}))} J_0(KR) \quad (93)$$

where J_0 is the Bessel's function of order zero. For comparison purposes, the zero-order, or flat-surface coherent intensity is plotted in Fig. 6a along with the first-order intensity pulse using the same parameters as in Fig 5a. In this example, the incident field is below the critical angle. Although the zero-order component can be approximated from Eq. (93) using the method of stationary phase to solve the resulting integral (see for example Brekhovskikh, 1980; Ishimaru, 1991) when the incident field is above the critical angle, a numerical method is more suitable when the incident grazing angle is close to critical (Westwood, 1989). The incident grazing angle is defined here to be the angle between the mean surface and the line containing the source and receiver points. Figure 6a shows an "exact" solution of the flat-surface intensity time series pulse, along with the first-order pulse (including dispersion terms) from Fig. 5a. For this example, the zero-order intensity pulse arrives earlier and with greater magnitude than the first-order pulse. In Fig. 6b, the source is moved further from the surface than the previous two examples. Even though the sediment parameters, receiver point, and incident angle are unchanged from Fig. 6a, the incoherent first-order intensity pulse is greater in magnitude than the zero-order intensity pulse. As the source is moved further from the surface, the stationary phase path for the zero order pulse is longer, and the zero-order pulse amplitude is more attenuated in the lossy sediment. Since Fig. 4 is a plane wave CW version of this same example, one would expect that the first-order intensity would be greater than the zero-order intensity for the source point sufficiently far from the surface.

VI. CONCLUSION

A general analytical expression for the time dependent narrowband scattered intensity from and through a fluid-fluid rough interface can be expressed in terms of the second moment of the T -matrix, or equivalently, in terms of the scattering cross section per unit area. For the special case of a CW incident plane wave, this result is exact, which is surprising as the scattering cross section is a far-field entity. Using first-order perturbation theory to obtain the scattering cross section per unit area yields a simple expression for the incoherent scattered time dependent intensity pulse. This expression is especially tractable when the source pulse is Gaussian.

The above formalism applied to the scattering through a rough surface shows the effect of roughness on penetration through a surface. When the grazing angle of a plane wave incident field is below the critical angle in relation to the mean surface, the zero-order component of the transmitted field is evanescent, and does not penetrate deeply into the seafloor. Higher order components contain downward traveling waves, which can increase the depth of penetration of sound relative to the flat-surface case.

ACKNOWLEDGMENTS

This work was supported by the Office of Naval Research. The authors are grateful to Dr. Eric Thorsos and Dr. Kevin Williams for useful technical discussions.

- Berman, D. H. (1992). "Renormalization of propagation in a waveguide with rough boundaries," J. Acoust. Soc. Am. **92**(1), 309-314.
- Brekhovskikh, L. M. (1980). *Waves in Layered Media* (Academic Press, San Diego), Chap 4.
- Devaney, A. J., Sherman, G. C. (1973). "Plane-wave representations for scalar wave fields," SIAM Rev. **15**, 765-786.
- Ishimaru, A. (1978). *Wave Propagation and Scattering in Random Media II* (Academic, San Diego), Chap. 21.
- Ishimaru, A. (1991). *Electromagnetic Wave Propagation, Radiation, and Scattering* (Prentice Hall, Englewood Cliffs), Chap. 4, Chap. 15.
- Moe, J. E., and Jackson, D. R. (1994a). "First order perturbation solution for rough surface scattering cross section including the effects of gradients," J. Acoust. Soc. Am. **96**(3), 1748-1754.
- Moe, J. E., and Jackson, D. R. (1994b). "The effect of roughness on acoustic penetration of the ocean bottom," J. Acoust. Soc. Am. **96**(5), 3265.
- Papoulis, Athanasios (1984). *Probability, Random Variables, and Stochastic Processes* (McGraw-Hill, New York), pg 273-274.
- Proakis, J. G. (1989). *Digital Communications* (McGraw-Hill, New York), Chap. 3.
- Rice, S. O. (1951). "Reflection of electromagnetic waves from slightly rough surfaces," Commun. Pure Appl. Math. **4**, 351-378.
- Thorsos, E. I., and Jackson, D. R. (1989). "The validity of the perturbation approximation for rough surface scattering using a Gaussian roughness spectrum," J. Acoust. Soc. Am. **86**(1), 261-277.
- Thorsos, E. I. (1990). "Acoustic scattering from a 'Pierson-Moskowitz' sea surface," J. Acoust. Soc. Am. **88**(1), 335-349.
- Voronovich, A. G. (1994). *Wave scattering from rough surfaces* (Springer-Verlag, Berlin), pg 33-36.
- Westwood, E. K. (1989). "Complex ray methods for acoustic interaction at a fluid-fluid interface," J. Acoust. Soc. Am. **85**(5), 1872-1884.
- Zipfel, G. G., and DeSanto, John A. (1972) "Scattering of a scalar wave from a random rough surface: a diagrammatic approach," J. Math Phys., vol. 13, No. 12.

APPENDIX: PERTURBATION THEORY RESULTS

The fields and T -matrices are expanded in their zero-order and first-order components, with the factor $k_1 h$ displayed explicitly:

$$\Psi(\mathbf{K}) = \Psi^{(0)}(\mathbf{K}) + k_1 h \Psi^{(1)}(\mathbf{K}) \quad (\text{A1})$$

$$T(\mathbf{K}, \mathbf{K}_i) = T^{(0)}(\mathbf{K}, \mathbf{K}_i) + k_1 h T^{(1)}(\mathbf{K}, \mathbf{K}_i) \quad (\text{A2})$$

Zero-order

The zero-order scattered field, or reflected field:

$$\Psi_f^{(0)}(\mathbf{K}) = \Gamma(\mathbf{K}) \Psi_i(\mathbf{K}) \quad (\text{A3})$$

where $\Gamma(\mathbf{K})$ is the flat-surface reflection coefficient,

$$\Gamma(\mathbf{K}) = \frac{\rho \beta_1(\mathbf{K}) - \kappa \beta_2(\mathbf{K})}{\rho \beta_1(\mathbf{K}) + \kappa \beta_2(\mathbf{K})} \quad (\text{A4})$$

Comparing Eq. (12) to (A3), the reflection coefficient is related to the zero-order T -matrix $T_{11}^{(0)}$ by:

$$T_{11}^{(0)}(\mathbf{K}, \mathbf{K}_i) = \Gamma(\mathbf{K}) \delta(\mathbf{K} - \mathbf{K}_i) \quad (\text{A5}).$$

The transmitted field is given in terms of the incident field and transmission coefficient,

$$\Psi_{2-}^{(0)}(\mathbf{K}) = \mathcal{T}(\mathbf{K}) \Psi_i(\mathbf{K}) \quad (\text{A6})$$

Comparing Eq. (13) with (A6), the transmission coefficient is related to the zero-order T -matrix $T_{12}^{(0)}$ by:

$$T_{12}^{(0)}(\mathbf{K}, \mathbf{K}_i) = \mathcal{T}(\mathbf{K}) \delta(\mathbf{K} - \mathbf{K}_i) \quad (\text{A7})$$

First-order

The first-order T -matrices are proportional to the 2-D Fourier transform of the surface, $F(\mathbf{K})$, and can be written as:

$$T_{11}^{(1)}(\mathbf{K}, \mathbf{K}_i) = H_{11}(\mathbf{K}, \mathbf{K}_i) F(\mathbf{K} - \mathbf{K}_i) \quad (\text{A8})$$

$$T_{12}^{(1)}(\mathbf{K}, \mathbf{K}_i) = H_{12}(\mathbf{K}, \mathbf{K}_i) F(\mathbf{K} - \mathbf{K}_i) \quad (\text{A9})$$

where,

$$F(\mathbf{K}) = \frac{1}{(2\pi)^2} \int d^2R f(\mathbf{R}) e^{-i\mathbf{K}' \cdot \mathbf{R}}. \quad (\text{A10})$$

From Moe and Jackson, (1994) Eqs. (26) and (29)

$$H_{11}(\mathbf{K}'', \mathbf{K}) = \frac{(1 + \Gamma(\mathbf{K}''))(1 + \Gamma(\mathbf{K}))}{2i\beta_1(\mathbf{K}'')} \times \left[1 - \frac{\kappa^2}{\rho} + \left(\frac{1}{\rho} - 1 \right) \left(\frac{\mathbf{K}'' \cdot \mathbf{K}}{k_1^2} - \rho\beta_1(\mathbf{K}'')\beta_1(\mathbf{K}) \frac{(1 - \Gamma(\mathbf{K}''))(1 - \Gamma(\mathbf{K}))}{(1 + \Gamma(\mathbf{K}''))(1 + \Gamma(\mathbf{K}))} \right) \right] \quad (\text{A11})$$

Since in the perturbation expansion (A1), the factor k_1 is displayed explicitly, the above expression is actually Eq. (29) of Moe and Jackson divided by a factor of k_1 . The following expression, equivalent to (A11), is convenient in the present problem:

$$H_{11}(\mathbf{K}'', \mathbf{K}) = \frac{1}{2i\beta_1(\mathbf{K}'')} \{ a(1 + \Gamma(\mathbf{K}''))(1 + \Gamma(\mathbf{K})) + b(1 - \Gamma(\mathbf{K}''))(1 - \Gamma(\mathbf{K})) \} \quad (\text{A12})$$

$$a(\mathbf{K}'', \mathbf{K}) = \left(\frac{1}{\rho} - 1 \right) \frac{\mathbf{K}'' \cdot \mathbf{K}}{k_1^2} + 1 - \frac{\kappa^2}{\rho} \quad (\text{A13})$$

$$b(\mathbf{K}'', \mathbf{K}) = \beta_1(\mathbf{K}'')\beta_1(\mathbf{K})(\rho - 1). \quad (\text{A14})$$

From Eq. (24) of Moe and Jackson (noting the difference in scalar field definitions, and no stratified media, $\Gamma_{23} = 0$), the continuity of pressure boundary condition for first-order fields yields:

$$\Psi_{2-}^{(1)}(\mathbf{K}'') = -i \int d^2K \Psi_i(\mathbf{K}) F(\mathbf{K}'' - \mathbf{K}) \quad (\text{A15})$$

$$\times \{iH_{11}(\mathbf{K}'', \mathbf{K}) + (1 - \Gamma(\mathbf{K}))\beta_1(\mathbf{K}) - \kappa\beta_2(\mathbf{K})(1 + \Gamma(\mathbf{K}))\}$$

Another expression for $\Psi_{2-}^{(1)}(\mathbf{K}'')$ follows from Eq. (13) and (A9)

$$\Psi_{2-}^{(1)}(\mathbf{K}'') = \int d^2K \Psi_i(\mathbf{K}) H_{12}(\mathbf{K}'', \mathbf{K}) F(\mathbf{K}'' - \mathbf{K}). \quad (\text{A16})$$

Equating (A15) and (A16) results in

$$H_{12}(\mathbf{K}'', \mathbf{K}) = H_{11}(\mathbf{K}'', \mathbf{K}) + (1 - \Gamma(\mathbf{K}))\beta_1(\mathbf{K}) + i\kappa\beta_2(\mathbf{K})(1 + \Gamma(\mathbf{K})). \quad (\text{A17})$$

Noting

$$\frac{\rho\beta_1}{\kappa\beta_2} = \frac{1 + \Gamma}{1 - \Gamma}, \quad (\text{A18})$$

(A17) simplifies to:

$$H_{12}(\mathbf{K}'', \mathbf{K}) = \frac{1}{i\sqrt{\rho}} \{iH_{11}(\mathbf{K}'', \mathbf{K}) + (1 - \rho)\beta_1(\mathbf{K})(1 - \Gamma(\mathbf{K}))\}. \quad (\text{A19})$$

Substituting (A12) into (A19) results in a useful expression for $H_{12}(\mathbf{K}'', \mathbf{K})$, given as Eq. (75).

FIGURE CAPTIONS

FIG. 1. Scattering problem geometry for rough interface separating a lossless fluid in medium 1 ($z > f(\mathbf{R})$), from a lossy fluid in medium 2 ($z < f(\mathbf{R})$). This diagram can be viewed as a slice through a 2-D surface.

FIG. 2. Diagram describing geometry of variables.

FIG. 3. Illustration of effect of dispersion on peak intensity. Peak of $g^2(t)$, normalized with respect to $\max(u^2(t))$ as a function of grazing angle.

FIG. 4. First-order and zero-order field strength as a function of depth. Field strength given in dB with respect to incident pressure. Critical angle is 27.75° , $f = 20 \text{ kHz}$, $a = 0.1 \text{ m}$, $\gamma = 3$, $w_2 = 2 \times 10^{-5} \text{ m}$, $\rho = 2$, $\delta = 0.019$, $c_1 = 1500 \text{ m/s}$, $\nu = 1.13$.

FIG. 5. Time-dependent intensity at depth 0.2 m below the mean surface. Source frequency = 20 kHz, $t_s = 100 \mu\text{s}$. Solid line: dispersion terms included; dotted line: dispersion terms set to zero, $g(t) = u(t)$. Same sediment parameters and incident angle as Fig. 4.

FIG. 6. Zero-order coherent time dependent intensity shown with dotted line, first-order incoherent intensity shown with solid line. All parameters identical to Fig. 5.

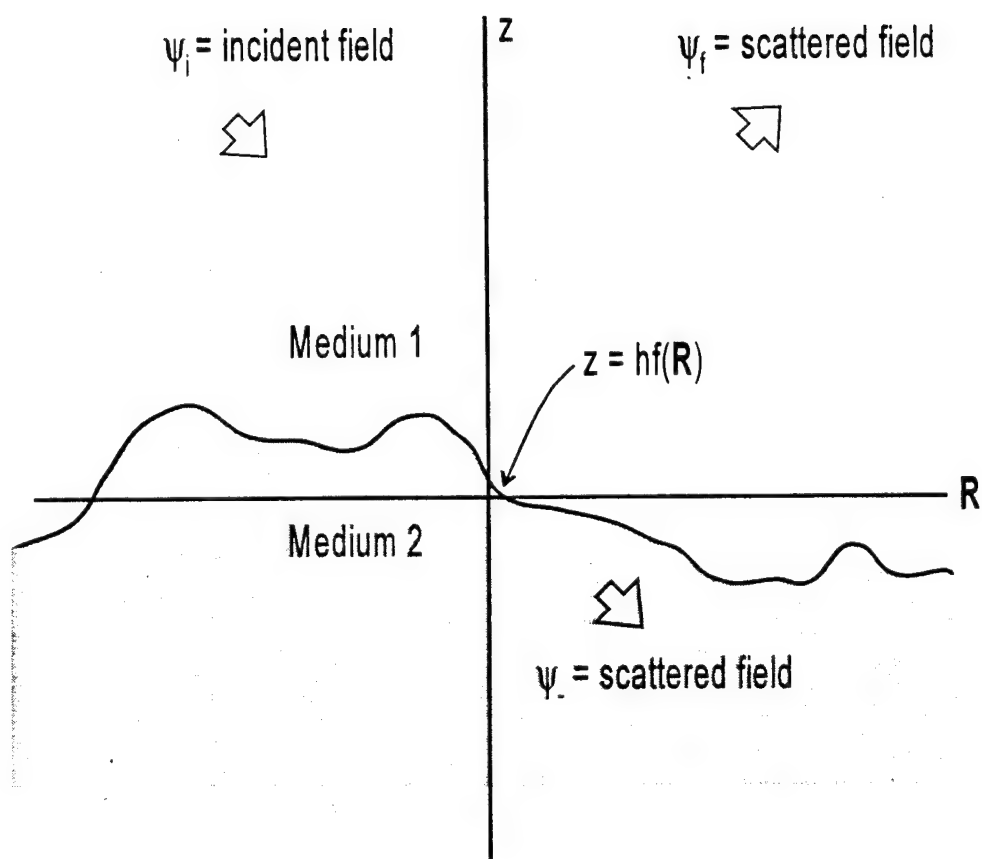


FIG 1

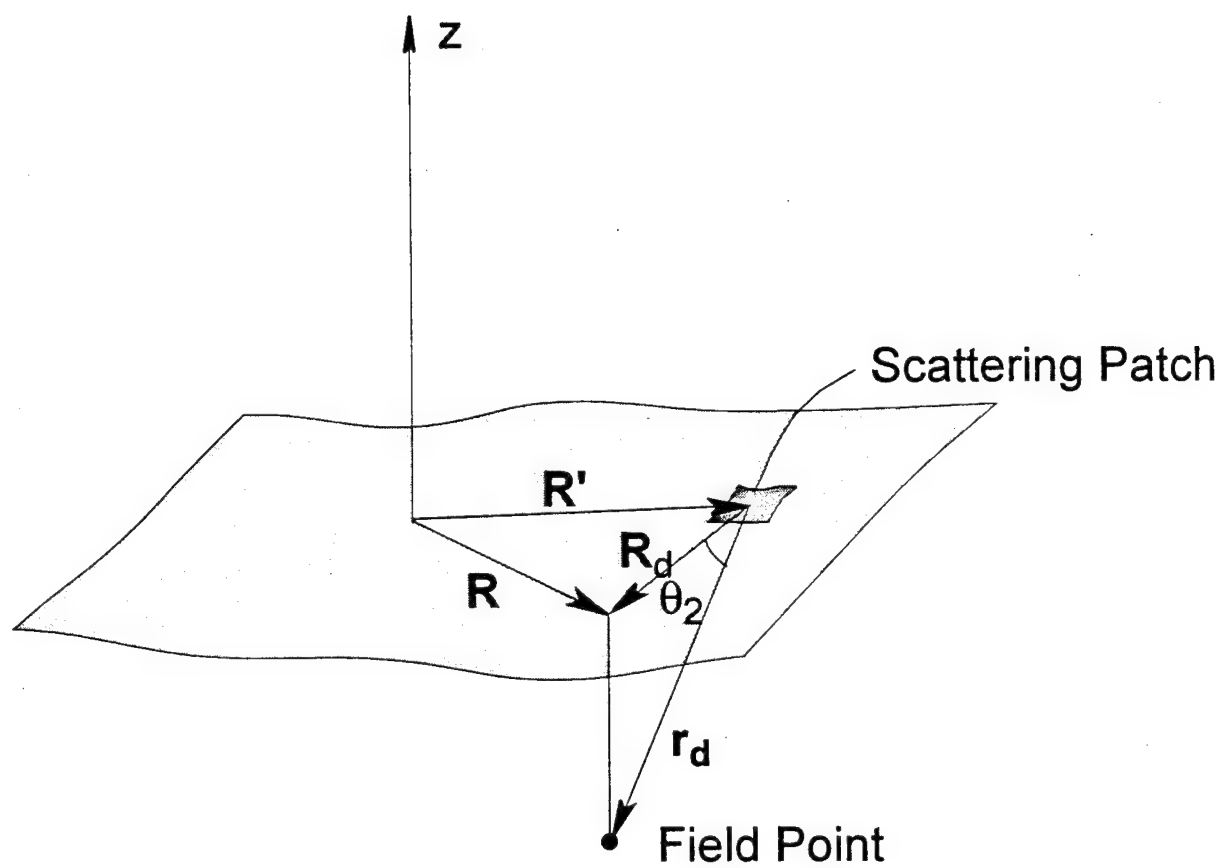
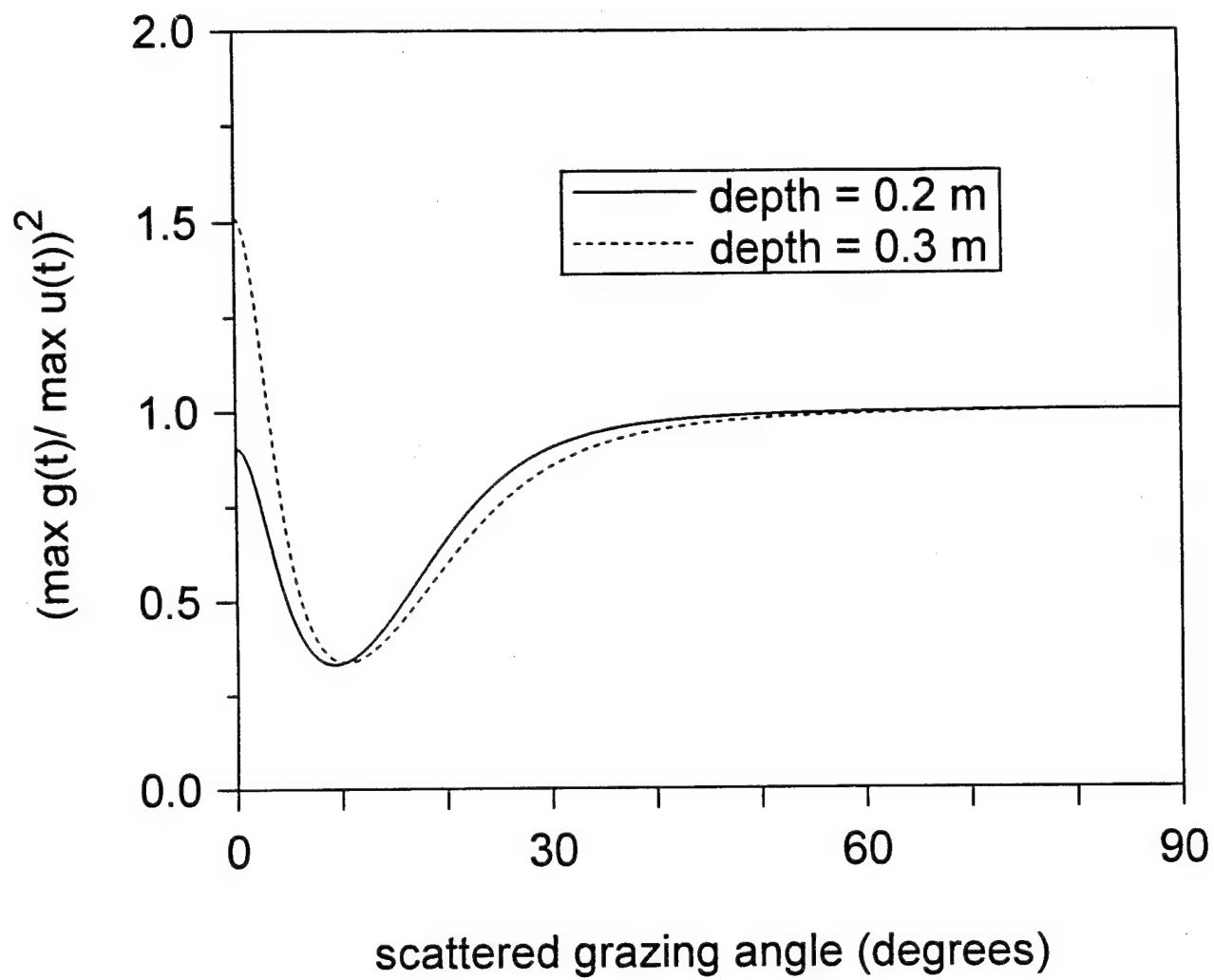


FIG 2



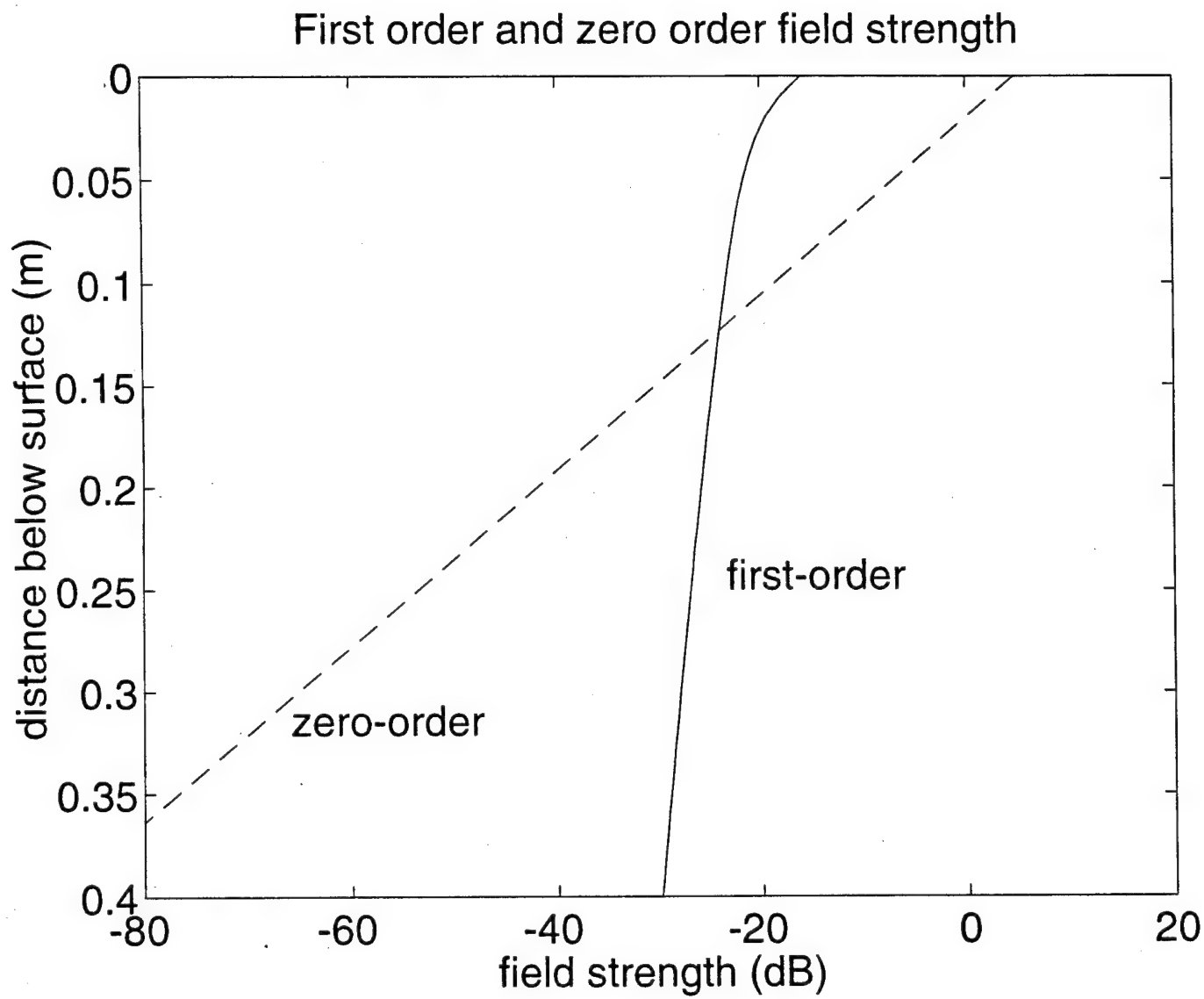


Fig 4

